World Academy of Science, Engineering and Technology
International Journal of Mechanical and Mechatronics Engineering
Vol:6, No:11, 2012

An Attempt to Predict the Performances of a Rocket Thrust Chamber

A. Benarous, D. Karmed, R. Haoui, and A. Liazid

***Abstract*—**The process for predicting the ballistic properties of a liquid rocket engine is based on the quantitative estimation of idealized performance deviations. In this aim, an equilibrium chemistry procedure is firstly developed and implemented in a Fortran routine. The thermodynamic formulation allows for the calculation of the theoretical performances of a rocket thrust chamber. In a second step, a computational fluid dynamic analysis of the turbulent reactive flow within the chamber is performed using a finite volume approach. The obtained values for the "quasi-real" performances account for both turbulent mixing and chemistry-turbulence coupling. In the present work, emphasis is made on the combustion efficiency performance for which deviation is mainly due to radial gradients of static temperature and mixture ratio. Numerical values of the characteristic velocity are successfully compared with results from an industry-used code. The results are also confronted with the experimental data of a laboratory-scale rocket engine.

***Keywords*—**JANAF methodology; Liquid rocket engine; Mascotte test-rig; Theoretical performances.

I. Introduction

CONVENTIONAL rocket engines for a launch vehicle need to deliver high thrust when taking off with the greatest vehicle weight. In this context, liquid propellant rocket engines (LRE's) provide good flexibility and better performances compared to any conventional chemical systems. This type of engines can be designed to be throttled and fired more than once in each mission. They are also highly controllable in terms of thrust modulation [1].

Assessing the performances of a rocket engine is of great importance in evaluating the overall performance of the entire propulsion system [2]. Because of the tremendous energy flow in LRE's, these engines are characterized by performance losses due to heat transfer, wall friction, incomplete vaporization and mixing inefficiencies [3].

The main objective of this work is to quantify performance losses in a laboratory-scale rocket engine [4]. According to the JANAF methodology, this task will be achieved in a two step procedure [5]. In a first step, performance expressions are derived by means of simple thermodynamics relations which allow for the calculation of the "theoretical" performances of the test-facility.

In a second step, a finite volume computation is performed on the chamber part of the subscale model, using the commercial software Ansys-Fluent [6]. As rocket engines are currently running at high chamber pressures, real-gas thermodynamics is mandatory to account for local mixing of propellants. In the present work we use a volume-weighted mixing rule for the mixture whereas the reactants are individually described by a Peng-Robinson equation of state (EOS) [7]. Both macro-mixing (EDM) [8] as well as Pdf-equilibrium models are used for the non premixed flame calculation.

For the purpose of comparison with the thermodynamic formulation, field values for the characteristic velocity (Cstar) are spatially averaged by means of a density weighted expression.

II. Thermochemical Analysis

Maximum performances of a thrust chamber sometimes called ideal or theoretical are achieved if the propellants react completely while a chemical equilibrium is maintained throughout the expansion process. Moreover, the flow within the nozzle should be isentropic and parallel to the divergent axis. Under these ideal conditions, analytic expressions for the thrust chamber performances can be derived [9].

A. Characteristic of the Combustion Products

For the purpose of evaluating the thermochemical characteristics of the products, it is important to quantify the enthalpy of the reactants. Indeed, the constant pressure assumption made on the combustion process implies the enthalpy conservation between the "fresh" reactants and the "burnt" products. At the injection state, the enthalpy of each propellant is given by:

$$H = Q^0_{(f,ox)} + H_{inj(f,ox)}$$
$$H_{inj(f,ox)} = -\left[\int_{T_{inj}}^{T_v} c_{p_{liq}}\, dT + L_v + \int_{T_v}^{T^*} c_p(T)\, dT\right]_{(f,ox)} \quad (1)$$

where T_{inj}, T_v, T^* denote respectively injection, vaporization and standard temperature of the propellant. Q^0 is the heat of formation and H_{inj} accounts for energy loss during the vaporization process. The fresh state of the mixture accounts

A. Benarous is with the Hassiba Benbouali University (UHB), Chlef, 02000 Algeria (phone: 00-213-662859251; fax: 00-213-27721794; e-mail: abenarous@ univ-chlef.dz).

D. Karmed, is with Pprime Institute, ENSMA, Poitiers University, Chasseneuil, 86961, France (e-mail: djamel.karmed@isae-ensma.fr).

R. Haoui is with the Advanced Mechanical Laboratory (LMA), Mechanics and Process Engineering Faculty, Houari Boumedienne University of Sciences and Technology (USTHB), Algiers, 16000, Algeria (e-mail: R.haoui@univ-usthb.dz).

A. Liazid is with the Environmental Technology Laboratory (LTE), Mechanical Department, ENSET High School, Oran, 31000, Algeria (e-mail: A. Liazid@enset.dz).

for both fuel and oxidizer enthalpies and relates on the flow rate of each propellant as:

$$H_u = \left(H_f + mrH_{ox}\right)/\left(1+mr\right) \quad (2)$$

where $mr = \dot{m}_{ox} / \dot{m}_f$ is the mixture ratio at the chamber inlet. According to the previous relations, basic equation of energy takes the following form:

$$H_u = \sum_{i=1}^{N} n_i(T_{ch}, P)\left[Q_i^0 + \int_{T^*}^{T_{ch}} c_{p_i}(T)dT \right] \quad (3)$$

where $n_i(T_{ch}, P)$ denotes a component of the composition vector at the chamber temperature.

Equation (3) is numerically solved to predict the adiabatic flame temperature (AFT) which is supposed to be equal to the chamber temperature. These two values are identical since we deal with a zero-dimensional thermodynamic approach.

When an equilibrium chemistry is maintained throughout the combustion process, contents of combustion products (n_i) are evaluated by means of a minimum Gibbs energy method [10].

Mean molecular weight and specific heat ratio of the mixture are respectively given by:

$$M = \frac{1}{n}\sum_{i=1}^{N} n_i M_i \ , \gamma = \frac{\sum_{i=1}^{N} n_i c_{p_i}}{\sum_{i=1}^{N} n_i c_{p_i} - r.\sum_{i=1}^{N} n_i} \quad (4)$$

where $r = R / M$ is the ideal gas constant.

B. Theoretical Performances Evaluation

A way of considering the contribution of the combustion chamber to the total thrust of the engine is to evaluate the characteristic velocity c^*. When the start-up and extinction transients are neglected, the theoretical Cstar value can be written as [9]:

$$c^*_{th} = \frac{P_{ch} A_t}{\dot{m}} = \frac{1}{\Psi(\gamma)}\sqrt{\frac{r.T_{ch}}{\gamma}} \quad (5)$$

with $\Psi(\gamma) = \left(\frac{2}{\gamma+1}\right)^{\frac{\gamma+1}{2(\gamma-1)}}$ (6)

As we deal with a thermochemical approach, specific heat ratio is taken to be equal to a fixed value which refers to the adiabatic flame temperature. Since it relates on T_{ch} / M ratio, the characteristic velocity is considered as an efficiency indicator for the combustion process.

Regarding the nozzle part of the thrust chamber, a second performance is defined. The thrust coefficient Cf represents the amount of thrust provided by the nozzle divergent [9]:

$$Cf_{th} = \Psi(\gamma)\sqrt{\frac{2}{\gamma-1}}\sqrt{1-(\delta_e)^{\frac{\gamma-1}{\gamma}}} + (\delta_e - \delta_a).\in_e \quad (7)$$

$\in_e = A_e / A_t$ denotes the exit area ratio and $\delta_e = P_e / P_{ch}$ is the expansion ratio.

The second term in the expression of the thrust coefficient accounts for non-adaptation effects noticed during flight conditions of a rocket engine. According to the test-rig operating conditions, the divergent exit pressure is often adapted to the ambient (sea-level) value. Consequently, the thrust coefficient is only related to the expansion ratio ($\delta_e = \delta_a$).

III. Computational Fluid Dynamic (CFD) Analysis

In this step, a CFD study is performed by solving the Favre averaged forms of the continuity, momentum, energy and species transport equations. The computational domain concerns the high pressure cryogenic combustor Mascotte V.03 [11]. The chamber is fed with a central liquid oxygen (LOx) surrounded by a gaseous hydrogen (Fig. 1a).

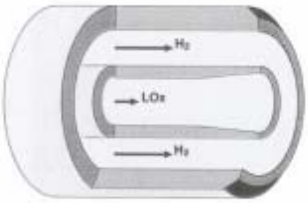

Fig. 1a Schematic view of the coaxial injector

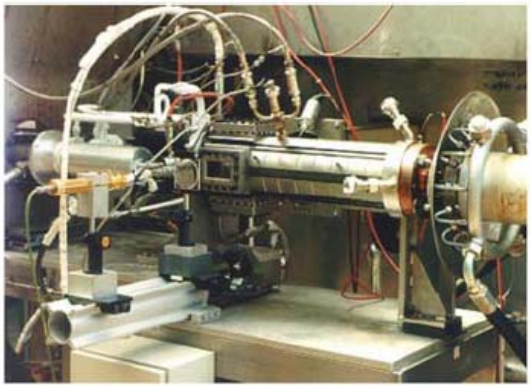

Fig. 1b The cryogenic combustor Mascotte [4]

The chamber shown in Fig. 1b is a square duct of 50 mm inner dimensions and a length of 458 mm. The nozzle of variable shape is mounted to maintain a constant pressure across the combustor. For the numerical investigations, the chamber was modeled rotationally symmetric with an equivalent diameter which reproduces the internal volume [12]. Velocities as well as turbulent profiles at the combustor inlet were obtained from a preliminary work regarding the cold-flow within the coaxial injector [13].

Owing to the lack of data regarding the supersonic flow, the

nozzle was not included in the computational domain (Fig. 2). The Mascotte rig operating conditions are depicted in Table I.

TABLE I
OPERATING CONDITIONS FOR RCM-3 TEST CASE

Operating conditions	H_2	O_2
Pressure [bars]	60	60
Temperature [K]	287	100
Mass flow rate [kg s^{-1}]	0.070	0.100
Injector inlet velocity [m s^{-1}]	236	4.35

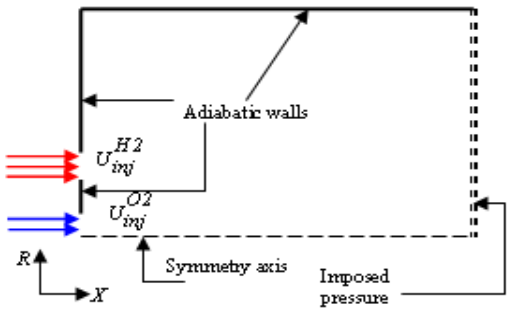

Fig. 2 The computational domain

It is obvious that we deal with a transcritical combustion regime since the chamber pressure exceeds the critical point of the liquid oxygen ($P_{crit} = 50.4$ bars) whereas the injection temperature is slightly below ($T_{crit} = 154$ K). For such situations, molecular transport properties, namely dynamic viscosity, thermal conductivity and species diffusion coefficients exhibit a considerable contribution on the mixing process [14]. In this work, the binary diffusion coefficient is described according to the Chapman-Enskog formulation [15] on which the Takahashi correction is made to account for high pressure regimes [16]. Viscosity and thermal conductivity are evaluated empirically using the correlation of Chung *et al.* [17]. Regarding the density, the Peng-Robinson (PR) equation of state is believed to be well suited for transcritical regimes [18]. The EOS is a three parameter formula accounting additionally for the deviation of molecules from the spherical shape. It has the following expression [7, 18]:

$$P = \frac{RT}{V-b} - \frac{a.\alpha(T)}{V^2 + 2bV - b^2} \tag{8}$$

with $a = a(T_{crit}, P_{crit}), b = b(T_{crit}, P_{crit})$

and $\alpha(T) = 1 + \delta(1 - \sqrt{T / T_{crit}})^2$ (9)

where δ is a function of the Pitzer's accentric factor of a pure species [7].

Keeping in mind that the standard $k-\varepsilon$ model overestimates mixing and turbulence level in axisymmetric jets [19], a limited Pope correction is made on the dissipation rate equation. As stated by Pope [20], the vortex stretching due to the round jets effects is modeled by adding a production term in ε transport equation of the plane-jet:

$$\frac{\partial}{\partial x_j}\left[\bar{\rho}\,\tilde{u}_j\,\tilde{\varepsilon}\right] = \frac{\partial}{\partial x_j}\left[\frac{\mu_t}{\sigma_\varepsilon}\frac{\partial \tilde{\varepsilon}}{\partial x_j}\right] + \frac{\tilde{\varepsilon}}{\tilde{k}}\left[C_{1\varepsilon}P_K - \bar{\rho}\,C_{2\varepsilon}\tilde{\varepsilon} + \bar{\rho}\,C_{3\varepsilon}\chi\,\tilde{\varepsilon}\right] \tag{10}$$

where $\chi = \omega_{ij}\omega_{jl}S_{li}$ is the vortex stretching factor and $\omega_{jl} = \frac{1}{2}\frac{\tilde{k}}{\tilde{\varepsilon}}\left[\frac{\partial \tilde{u}_j}{\partial x_l} - \frac{\partial \tilde{u}_j}{\partial x_l}\right]$, $S_{li} = \frac{1}{2}\frac{\tilde{k}}{\tilde{\varepsilon}}\left[\frac{\partial \tilde{u}_i}{\partial x_l} + \frac{\partial \tilde{u}_l}{\partial x_i}\right]$, with $C_{3\varepsilon}$ is a strictly positive constant. The correction is practically done by imposing a new value for the $C_{2\varepsilon}$ constant in a way that $C_{2\varepsilon}^{'} = C_{2\varepsilon} - \chi \cdot C_{3\varepsilon}$.

In the non premixed combustion cases, the algebraic approaches for the reaction rate expressions are mainly based on the works of Magnussen *et al.* [8]. In this linear relaxation model (EDM i.e. Eddy Dissipation Model), the chemical reactions are fully controlled by the turbulent macro-mixing.

Here, the large eddies tend to bring back fuel and oxidizer to a reaction zone situated within the mixing layer of the two reactant streams. The fuel reaction rate is proportional to the inverse of the turbulent eddy time scale:

$$\bar{\omega}_f = -\bar{\rho}.C_{Mag}\frac{\tilde{Y}_{H2}^{(0)}}{\tilde{k}/\tilde{\varepsilon}}Min\left(\tilde{Y}_{H2}, \tilde{Y}_{O2}/s, \tilde{Y}_{H2O}/1+s\right) \tag{11}$$

where C_{Mag} is an empirical constant and s is a mass stoichiometric ratio for the complete reaction of H_2 in O_2 ($s = 8$).

As it is stated in the previous model, chemical kinetics are not considered. Hence, only global chemistry calculations can be performed. To account for intermediate species (OH, HO_2, H,O,….), it is possible to use a stochastic approach based on a conserved scalar; i.e., the mixture fraction [21]. Here a transport equation for the passive scalar is solved and individual component concentrations are derived from a mixture fraction distribution. Turbulence-chemistry coupling effects are accounted for by means of a presumed probability density function (Pdf) which is supposed to follow a Beta shape [6].

IV. Results and Discussion

On a basis of the thermodynamic formulation a computer program was developed in the aim of providing the theoretical performances. The subscale rocket engine Mascotte has been chosen as a validation case [4]. For the present operating point (A60), the mixture ratio $mr = 1.42$ is maintained at the chamber inlet. Values for the chamber area ratio $A_{ch}/A_t = 22.4$ as well as the exit area ratio $A_e/A_t = 11.24$ are mandatory to run the computer procedure.

The obtained performances (Table II) are compared to those of the common-used industry Chemical Equilibrium and Applications code (CEA), developed by Gordon and Mc Bride at the NASA Glenn research centre [10].

TABLE II
CALCULATED ROCKET PERFORMANCES

Rocket performance	Computed value	CEA calculation	Deviation
Adiabatic flame temperature [K]	3693	3549.8	+4.03%
Characteristic velocity [m/s]	2341	2323	+0.77%
Thrust coefficient	1.681	1.658	+1.39%
Chamber-end static pressure [bars]	59.91	59.85	+0.10%

In Table II, a comparative study for the rocket performances values is provided. Excellent agreement is obtained between the developed computer program and CEA equilibrium code, with a maximum relative deviation of 4% noticed on the adiabatic flame temperature. The slight difference may be attributed to the trace elements (HO_2, H_2O_2, O, H) formed in CEA and not considered in our computations.

Regarding the rocket performances, there are no available experimental data for the Mascotte-rig, except at the chamber-end section where the probe indicates a centerline static pressure P_{ch} = 59.5bars. Accordingly, both CEA and the computer program seem to underestimate the static pressure loss across the combustion chamber.

In the following, particular attention will be paid on the evolution of the oxygen mass fraction. Indeed, because of the important density the radial spreading of the oxygen jet is considered as a yardstick of the local mixing. Here a CFD analysis of the flow without chemical production is performed.

The empirical constant $C_{2\varepsilon}$ of the turbulence model is adjusted to a value 1.87 so that the experimental oxygen mass fraction can be recovered. Fig. 3a and 3b show the radial profiles of the oxygen mass fraction at two axial stations $X/D = 2$ and $X/D = 50$

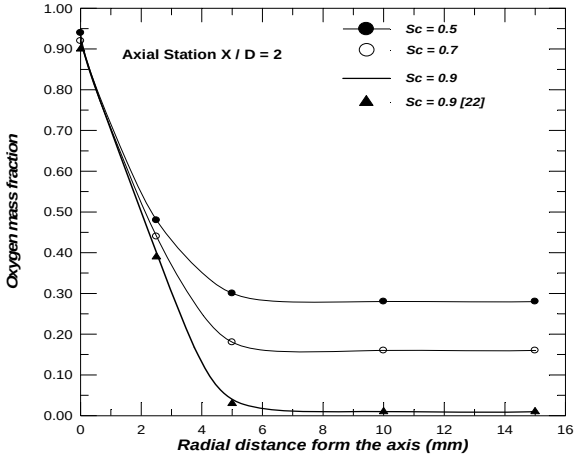

Fig. 3a Profiles of the oxygen mass fraction at 10 mm from the faceplate.

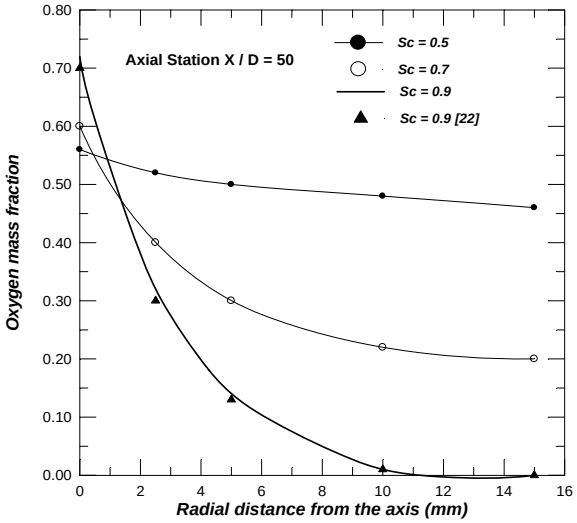

Fig. 3b Profiles of the oxygen mass fraction at 250 mm from the faceplate.

In the vicinity of the faceplate ($X/D = 2$), oxygen mass fraction shows an asymptotic tendency which reveals the existence of a recirculation zone where the oxygen is trapped.

The curve with $Sc_t = 0.9$ seems to fit quite well the measurements of Schmidt *et al.* [22] (Fig. 3a). In this zone, the turbulent diffusions is believed to be unimportant near the centerline since the predicted oxygen mass fractions are identical whatever the value of the turbulent Schmidt number.

When moving downstream the faceplate ($X/D = 50$) an important sensitivity of Y_{O2} to Schmidt number variations is noticed (Fig. 3b). Oxygen mass fraction exhibits an important decrease in the radial direction which will eventually lead to significant fluctuations of the local mixture ratio. It is important to notice that the experimental oxygen mass fraction is globally well fitted for a high Schmidt number value ($Sc_t = 0.9$) and this, whatever the value of the axial distance from the faceplate.

Regarding the hot fire simulation, the two chemistry-turbulence coupling models, namely the eddy dissipation (EDM) and the Pdf-Equilibrium were performed. The corresponding evolution of the centerline static temperature is depicted in Fig. 4.

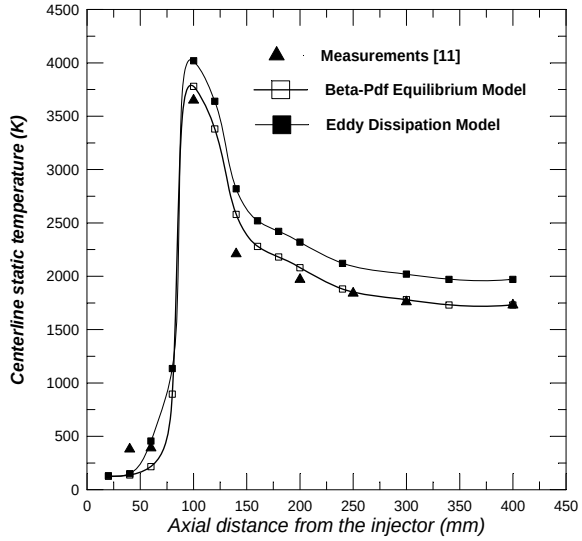

Fig. 4 Axial temperature profiles for various chemistry models

Fig. 4 clearly shows that the EDM model leads to a huge axial temperature for which the overestimation is about 14% compared with the measurements [11]. Moreover, the maximum temperature for this complete combustion model exhibits an important value (4020K) that exceeds the thermochemical threshold. However, the static temperature profile is quite close to the experiments when the β-Pdf equilibrium model is used. Here, the experimental temperature peak is overestimated by only 2.2%. Indeed, adopting the same number and type of species (H_2, O_2, H_2O, OH, O, H) as for the Euklund reduced scheme [23] will eventually account for enthalpy losses by dissociation. The equilibrium model also succeeds in yielding the thermal relaxation while fitting well the measurement points. The predicted temperature profile exhibits an asymptotic tendency beyond the axial station $X / D = 50$.

Since the degree of local mixing is related to the oxygen mass fraction, mixture ratio fluctuation will induce an enthalpy gradient while affecting the local heat release. In this case, static temperature as well as density may depend on the radial location so that the characteristic velocity is expressed with a mass-weighted averaging, as:

$$c^* = \sqrt{r}\,\frac{\int_{A250} \rho(T)\sqrt{T/(\gamma.\Psi^2(\gamma))}\; dA}{\int_{A250} \rho(T)\, dA} \qquad (12)$$

where A250 denotes the vertical plane $X = 50D = 250$ mm within the computational domain.

According to whether the mixture ratio is fixed to its injection value or considered as spatially variable, three various cases regarding Cstar calculations can be distinguished. The corresponding situations are depicted in Table III.

TABLE III
CASES CONSIDERED IN CSTAR EVALUATION

	Case #1	Case #2	Case #3
Mixture ratio	Bulk value 1.428	Spatially variable $mr(R)\big\|_{X=250\,\mathrm{mm}}$	Spatially variable $mr(R)\big\|_{X=250\,\mathrm{mm}}$
Chemical reaction	Equilibrium reactions (6 species)	One step reaction (3 species)	Equilibrium reactions (6 species)
Chemistry-turbulence coupling	-------	Eddy Dissipation model	β-Pdf equilibrium model
Chamber temperature [K]	Bulk value 3693	Spatially variable $T(R)\big\|_{X=250}$	Spatially variable $T(R)\big\|_{X=250}$

For each of the three cases, number and type of chemical species are related to the adopted chemistry mechanism.

Moreover, turbulence-chemistry coupling determines the expression of the chemistry source term and consequently accounts for spatial gradients of fuel and oxidizer mass fractions. Case #1 is an application of the thermochemical procedure to the Mascotte's operating point (A60). Here, the computations are performed for a fixed value of the mixture ratio and a bulk chamber temperature. Accordingly, a maximum value for the characteristic velocity is expected to be reached in this ideal case. The remaining cases (case #2, case #3) are based on CFD calculations and use the integral averaging of the characteristic velocity (equation (12)).

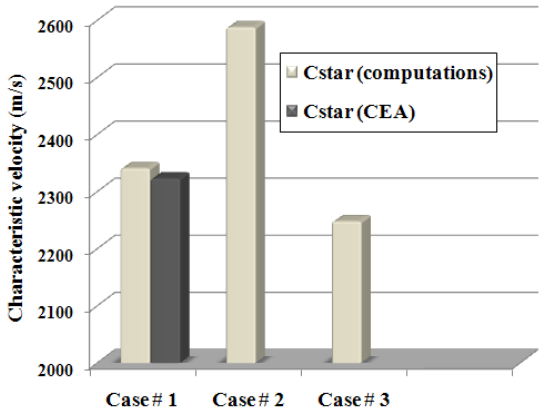

Fig. 5 Characteristic velocity comparisons

Fig. 5 provides the comparative charts for the computed characteristic velocity for the three examined cases. Good agreement is obtained between the two procedures (computer program and CEA code) for case #1. The minor overestimation of 0.77% is a consequence of the thermal discrepancy between the thermochemical calculations.

In case #2, the obtained characteristic velocity exceeds its ideal value ($c^*_{th} = 2341\,m/s$) despite a good prediction of the oxygen mass fraction in the cold-flow calculations. Hence, the eddy dissipation model largely overestimates the static temperature and yields consequently a non-realistic Cstar

index ($\eta_{Cstar} = 110\,\%$). The characteristic velocity loss seems to be more reasonable for the β-pdf equilibrium model (case #3) with an efficiency index of $\eta_{Cstar} = 96\,\%$. The corresponding characteristic velocity $c^* = 2248\,m/s$ is slightly lower than its ideal value. This result further confirms that the Pdf-equilibrium chemistry is well suited to describe the reactive flow within the chamber part of a liquid rocket engine.

V. Conclusion

For the purpose of predicting the performances of liquid rocket engines, a two-step procedure was performed. It consists in joining an analytical formulation for the ideal performances to a CFD-based calculation. An emphasis is made on the combustion efficiency within a subscale model of a liquid rocket engine. The thermochemical procedure allows for the estimation of the maximum characteristic velocity for which the value was quite close to CEA calculations.

Experimental profiles of the oxygen mass fraction were successfully recovered thanks to a limited Pope correction made on the $k-\varepsilon$ turbulence model. The calculations have confirmed that the eddy time scale expression for the fuel reaction rate was inappropriate to predict the thermal level within the combustion chamber. However, the presumed-Pdf equilibrium model has been shown to perform excellent agreements with experiments for both cold-flow and hot-fire calculations. Detailed experimental data regarding the chamber region will provide further model validation and predictive-tool developments.

Acknowledgment

The authors would like to thank the Centre National de la Recherche Scientifique (C.N.R.S.) – France, for providing technical data. A. Benarous and R. Haoui were funded by the General Committee of Scientific Research and Technological Development (DGRSDT) – Algeria under contract PNR/15/U160/1142/2011.

References

[1] P. Caisso, *et al* ., "A Liquid propulsion panorama," *Acta Astronautica,* vol. 65, pp.1723-1737, 2009.

[2] G. Cai, J. Fang, X. Xu, and M. Liu, "Performance prediction and optimization for liquid rocket engine nozzle," *Aerospace Science and Technology,* vol. 11, pp.155-162, 2007.

[3] S.S. Dunn, and D.E. Coats, "Nozzle performance predictions use the TDK-97 code," *AIAA paper* 97-2807, 1997.

[4] M. Habiballah, *et al.,* "Experimental studies of high pressure cryogenic flames on the Mascotte facility," *Combustion Science and Technology,* vol. 178, pp.101-128, 2006.

[5] JANAF, "Rocket Engine Performance Prediction and Evaluation," *CPIA* 246, April 1975.

[6] Ansys-Fluent Software, Ver.6.2.16, Lebanon, NH, USA, 2005.

[7] D.Y. Peng, and D.B. Robinson, "A new two-constant equation of state," *Industrial Engineering Chemistry and Fundamentals* vol. 15, no.1, pp.59-63, 1976.

[8] B.F. Magnussen, and B.H. Hjertager, "On mathematical models of turbulent combustion with special emphasis on soot formation and combustion," *In Proceedings 16th International Symposium on Combustion*, The Combustion Institute, Pittsburg, Penn., 1976, pp. 719-729.

[9] G.P. Sutton, Rocket Propulsion Elements: An Introduction to the Engineering of Rockets. London: Wiley Interscience Publishing, 1986, ch. 3.

[10] S. Gordon, and B.J. Mc Bride, "Computer program for calculation of complex chemical equilibrium compositions and applications," *NASA Reference Publication,* no.1311, Lewis Research Center, Cleveland, OH,1994.

[11] J.L. Thomas, and S. Zurbach, "Test case RCM3: supercritical spray combustion at 60 bars at Mascotte," *in Proceeding of the 2nd International Workshop on Rocket Combustion Modeling*, Lampoldhausen, Germany, 2001, pp.13-23.

[12] M.M. Poschner, and M. Pfitzner, "Real gas CFD simulation of supercritical H_2-LOX combustion in the Mascotte single-injector combustor using a commercial CFD code," *AIAA Paper,* 2008-952 2008.

[13] A. Benarous, A. Liazid, and D. Karmed, "H_2/O_2 combustion under supercritical conditions," *In Proceeding of the 3rd European Combustion Meeting*, Creete, Greece, 2007, pp.156-161.

[14] V. Yang, "Modeling of supercritical vaporization, mixing and combustion processes in liquid- fueled propulsion systems," *The Combustion Institute,* vol. 28, pp. 925-942, 2000.

[15] S. Chapman, and T.G. Cowling, The Mathematical Theory of Nonuniform Gases. London: Cambrigde University Press, 1952, ch. 8.

[16] S. Takahashi, "Preparation of a generalized chart for the diffusion coefficients of gases at high pressures," *Journal of Chemical Engineering in Japan*, vol. 7, no.6, pp. 417-420, 1974.

[17] T.H. Chung, M. Ajlan, L.L. Lee, and K.E. Starling, "Generalized multiparameter correlation for non polar fluid transport properties," *Industrial and Engineering Chemistry Research*, vol. 27, no.4, pp.671-679, 1988.

[18] K. G. Harstad, R.S. Miller, and J. Bellan, "Efficient high pressure state equations," *AIChE Journal,* vol. 43, no.6, pp. 1605-1610, 1997.

[19] B.E. Launder, and D.B. Spalding, "The numerical computation of turbulent flows," *Computational Methods in Applied Mechanical Engineering,* vol. 3, pp.269-289, 1974.

[20] S.B. Pope, "An explanation of the turbulent round-jet/plane-jet anomaly," *AIAA Journal, vol. 16, no.3,* pp. 279-281, 1978.

[21] T. Poinsot, and D. Veynante, *Theoretical and Numerical Combustion*, Philadelphia: R. T. Edwards Editions, 2005, ch. 3.

[22] V. Schmidt, *et al.* "Experimental investigation and modeling of the ignition transient of a coaxial H_2/O_2 injector," In *Proceedings 5th International Symposium on Space Propulsion*, Chattanooga, Tenn., 2003, pp. 8 – 36.

[23] D. Gaffie, *et al.*, "Numerical investigation of supersonic reacting hydrogen jets in a hot air co-flow," *AIAA Paper*, 01-1864, 2001.

A. Benarous was born in Chlef, Algeria in 1971. He received aeronautics and space engineering degree from Blida University, Algeria in 1995 and a master degree in mechanical engineering from Chlef University, Algeria in 2002. The degree of Ph.D in aero-mechanical engineering was received from Oran University of sciences and technology, Algeria in 2010.

Since 2002, he is teaching as an Associate Professor at Chlef University. He is also considered as a Permanent Researcher at the LTE laboratory, Oran.

From 2008 to 2010, Dr Benarous joined the combustion team of Pr M. Champion (ENSMA, France) as a doctoral candidate.

Dr. Benarous is currently working on supercritical thermodynamics and turbulent combustion modeling in liquid rocket engines.